



## Template-directed excimer formation *via* specific non-covalent interactions between pyrene guanidinium derivatives and nucleic acids

Karen Amirbekyan<sup>a,b</sup>, Justine Mansot<sup>a</sup>, Keiichiro Ohara<sup>a</sup>, Shiraz A. Markarian<sup>b</sup>, Jean-Jacques Vasseur<sup>a</sup>, Michael Smietana<sup>a,\*</sup>

<sup>a</sup> Institut des Biomolécules Max Mousseron, UMR 5247 CNRS, Université de Montpellier, ENSCM, Place Eugène Bataillon, 34095 Montpellier, France

<sup>b</sup> Department of Physical Chemistry, Yerevan State University, 1 Alex Manoogian, Yerevan 0025, Armenia

### ARTICLE INFO

#### Article history:

Received 9 October 2017

Revised 4 December 2017

Accepted 12 December 2017

Available online 13 December 2017

#### Keywords:

Excimer fluorescence

Pyrene

Nucleic acids

G-quadruplex

### ABSTRACT

Structurally distinct guanidinium derivatives were evaluated for their ability to interact non-covalently with various nucleic acid sequences. Among the evaluated derivatives, 4-[(pyrene-1-ylmethyl)amino]butyl] guanidinium (**pbg**) was found to demonstrate strong excimer emission upon nucleic acid addition and high levels of discrimination between ds- and ss-DNA. The intensity of excimer emission proved to be dependent on the length of the linker probe as well as the oligonucleotide length and sequence. In particular, G-quadruplex prone structures were found to induce the highest excimer emissions among all nucleic acids tested.

© 2017 Elsevier Ltd. All rights reserved.

Pyrene is undoubtedly one of the most useful proximity reporters in sensor design owing to its exceptional excimer forming ability. Typically, the monomer emission is characterized by well-defined peaks at ~370–380 nm which differs from the broad band at 450–500 nm observed when two pyrene rings are brought into close proximity. This feature has notably been used for sensing metal ions, phosphates<sup>1</sup> and biomolecules.<sup>2–4</sup> In particular, pyrene excimer fluorescence has proved to be extremely useful in the context of DNA sensing. In a large number of these studies the pyrene moiety is incorporated covalently into DNA sequences through the use of modified phosphoramidite units or post-synthetic modifications.<sup>5–9</sup> Non-covalent approaches have also been evaluated by exploiting electrostatic interactions between positively charged pyrene derivatives and negatively charged phosphodiester internucleosidic linkages of DNA or RNA.<sup>10–16</sup> Interestingly, it has been demonstrated by fluorescence studies that pyrene-ammonium, pyrene-imidazolium and pyrene-thiazolium derivatives induce large excimer/monomer intensity ratios in the presence of G-quadruplex structures.<sup>10,11,14–16</sup> Our interest in positively charged pyrene derivatives was originally stimulated by a desire to characterize non-covalently bound complexes of guanidinium receptors and single-stranded DNA by matrix-assisted laser desorption/ionization (MALDI) mass spectrometry.

This study revealed the importance of hydrophobicity and  $\pi$ - $\pi$  stacking interactions and highlighted the prevalence of the pyrene moiety to form very strong complexes with DNA.<sup>17</sup> These properties were eventually extended to the analysis of sulfated polysaccharides and sulfopeptides.<sup>18,19</sup> In light of these results we decided to evaluate the extent of excimer formation between guanidinium derivatives and ssDNA or ssRNA. This study will thus consolidate our ongoing work devoted to evaluate the Y-shape electrostatic interactions between guanidinium and phosphodiester internucleosidic linkages.<sup>20</sup> In order to identify the structural elements that favor excimer emission, 1-pyrenemethyl guanidinium (**pmg**), [4-[(pyrene-1-ylmethyl)amino]butyl] guanidinium (**pbg**), and [6-[(pyrene-1-ylmethyl)amino]hexyl] guanidinium (**phg**) were synthesized as previously reported<sup>20</sup> and evaluated in the presence of homo- and heteropolymeric DNA or RNA oligonucleotides of different lengths (Fig. 1).

The UV–Vis spectra of **pmg**, **pbg** and **phg** show that for a fixed concentration of each guanidinium derivative (50 and 100 mM), addition of an increasing amount of the heteropolymeric random sequence poly(dN<sub>25</sub>) (5'-AGCTCGTTTAGTGAACCGTCAGATC-3') led to a decrease of the absorption bands of the pyrene units at 310, 330 and 340 nm, thus suggesting strong interactions between the oligonucleotide and the guanidinium moiety (Fig. 2). Based on these titrations curves the binding constants of **pmg**, **pbg** and **phg** were found to be  $5.53 (\pm 0.15) \times 10^5$ ,  $4.70 (\pm 0.12) \times 10^5$  and  $3.95 (\pm 0.10) \times 10^5 \text{ M}^{-1}$ , respectively (ESI). These results indicate the preferential binding of **pmg** and **pbg** over the more flexible

\* Corresponding author.

E-mail address: [michael.smietana@umontpellier.fr](mailto:michael.smietana@umontpellier.fr) (M. Smietana).

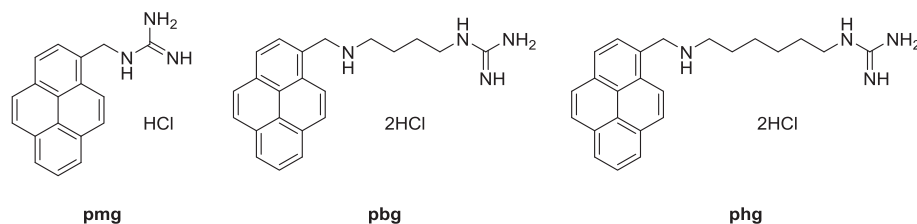


**Fig. 1.** Structures of the evaluated pyrene-guanidinium derivatives.

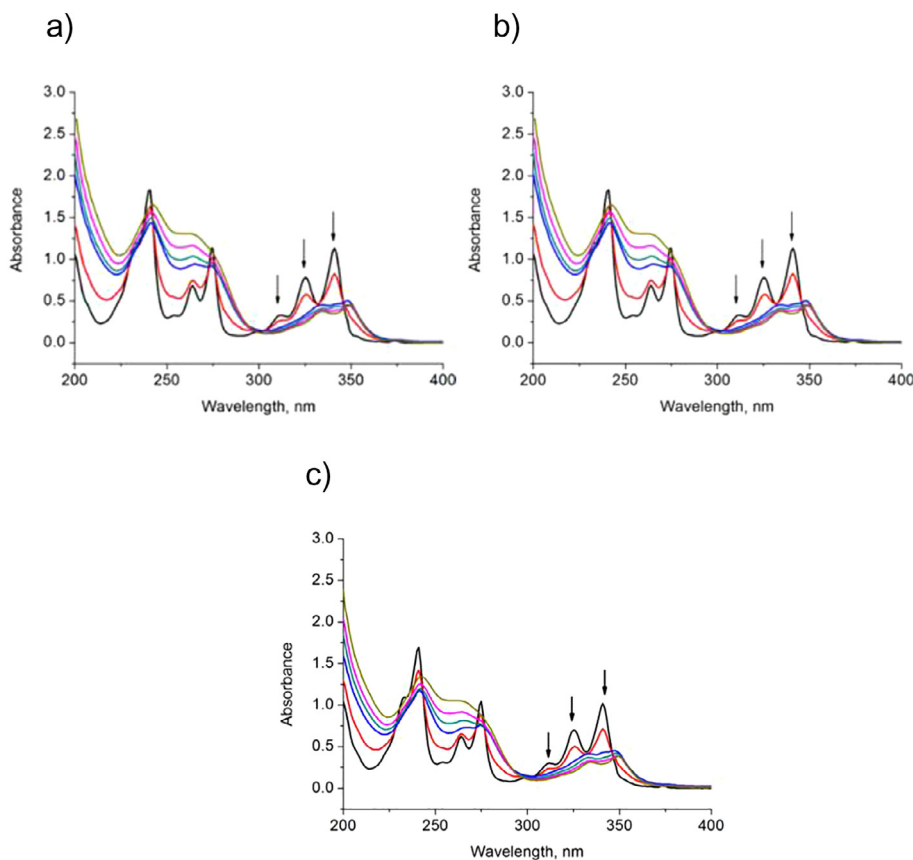


**Fig. 2.** UV-vis absorption spectra of a) **pmg**, b) **pbg** and c) **phg** titrated with poly(dN)<sub>25</sub>. Downward arrows show a decrease in absorbance upon interaction with poly(dN)<sub>25</sub>. Experiments were performed in MOPS buffer (1 mM MOPS and 1 mM NaCl) at pH = 7.5.

**phg** and the slight influence of the added positive charge carried by **pbg** and **phg**.

We then evaluated the fluorescence changes upon titration of **pmg**, **pbg** and **phg** (50 and 100  $\mu$ M) with increasing amounts of homo- and heteropolymeric DNA oligonucleotides of different lengths. For all oligonucleotides the spectra showed a decrease of the monomer emission (at 375 and 395 nm) concomitant with the appearance of a red-shifted emission band at 470 nm characteristic of pyrene excimer emission. In all cases, as the concentration of DNA was augmented the excimer/monomer emission ( $I_E/I_M$ ) increased up to a maximum point before it started to decrease.

As a general trend higher  $I_E/I_M$  maximum values were obtained when the concentration of the guanidinium probe was fixed at 100  $\mu$ M. Interestingly, the relative intensity of the pyrene excimer emission was highly dependent on the spacer length. As can be seen in Fig. 3, **pmg** which has the shortest alkyl linker (methyl), demonstrates low excimer emission compared to the aminobutyl and aminohexyl linkers. The lower flexibility for stacking interactions imposed by the methylene linker might explain this observation.

Meanwhile, with longer linkers, charge repulsion does not seem to inhibit excimer formation. The  $I_E/I_M$  maximum value was also strongly dependent on the DNA sequence especially for **pbg** and **phg**. Poly

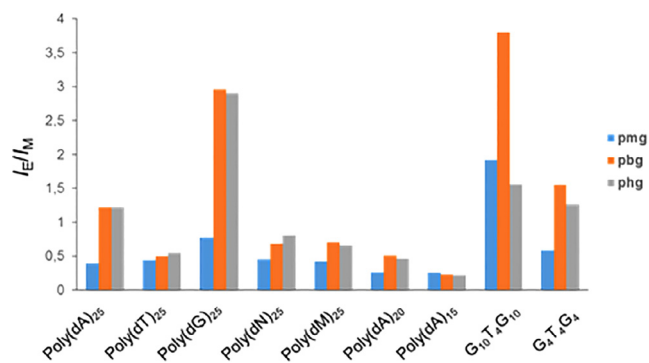


**Fig. 3.**  $I_E/I_M$  maximum values obtained for **pmg**, **pbg** and **phg** (100  $\mu$ M) mixed with various DNA sequences. Experiments were performed in MOPS buffer (1 mM MOPS and 1 mM NaCl) at pH = 7.5.

(dA)<sub>25</sub> and poly(dT)<sub>25</sub> were found to induce excimer formation, while in the presence of poly(dC)<sub>25</sub> no excimer could be detected. Random hetero sequences poly(dN)<sub>25</sub> and poly(dM)<sub>25</sub> (5'-GATCTGACGGTTCCTAAACGAGCT-3') also gave an excimer formation with  $I_E/I_M$  values in the range of homogeneous poly(dA)<sub>25</sub> and poly(dT)<sub>25</sub>. Furthermore, our results show that shortening the nucleic acid length reduces excimer formation. Excimer formation was weak for poly(dA)<sub>20</sub> and poly(dA)<sub>15</sub> compared to poly(dA)<sub>25</sub>, while for poly(dA)<sub>10</sub> and poly(dA)<sub>5</sub> excimer formation could not be detected. Interestingly, higher  $I_E/I_M$  values were observed with poly(dG)<sub>25</sub>. On the basis of the UV titration curves, the binding constants of the **pbg**/DNA complexes were determined by Scatchard analysis to be:  $15.60 \times 10^5$  for poly(dA)<sub>25</sub>,  $1.48 \times 10^5$  for poly(dT)<sub>25</sub>,  $8.80 \times 10^5$  for poly(dC)<sub>25</sub> and  $5.93 \times 10^5$  for poly(dG)<sub>25</sub>. Binding constants obtained by plotting the fraction of bound **pbg** vs DNA concentration led to a similar trend (see ESI). Analysis of these results reveals that there is no linear correlation between the binding constant and the  $I_E/I_M$  values, thus indicating the importance of the structural features of the templating nucleic acid. These results prompted us to evaluate well-known G-quadruplex prone sequences G<sub>10</sub>T<sub>4</sub>G<sub>10</sub> and G<sub>4</sub>T<sub>4</sub>G<sub>4</sub>.<sup>21–25</sup> In the presence of these sequences  $I_E/I_M$  maximum values were dramatically enhanced even in the presence of **pmg**, thus demonstrating the ability of G-quadruplex structures to organize the assembly of the pyrene units and to promote  $\pi$ - $\pi$  stacking interactions. The highest  $I_E/I_M$  value was obtained with 24-mer G<sub>10</sub>T<sub>4</sub>G<sub>10</sub> (Fig. 4), but even the shorter oligonucleotide 12-mer G<sub>4</sub>T<sub>4</sub>G<sub>4</sub> induces high excimer formation (see ESI).

Finally, the lowest amount of DNA concentration to reach the maxima was always obtained with poly(dA)<sub>25</sub> (4.2, 5.6 and 4.2  $\mu$ M for **pmg**, **pbg** and **phg**, respectively) while 14.0, 21.0 and 18.2  $\mu$ M of G<sub>4</sub>T<sub>4</sub>G<sub>4</sub> were respectively needed (Table S1). These values also indicate that there is no direct correlation between the

molar ratio of positive charges carried by the probes and the negatively charged phosphodiester linkages.

The CD spectra of poly(dG)<sub>25</sub> and G<sub>10</sub>T<sub>4</sub>G<sub>10</sub> in MOPS buffer (pH 7.5) in the presence of **pbg** are shown in Fig. 5. It is well documented that the antiparallel G-quadruplex structure has a positive peak near 295 nm and a negative peak near 265 nm in the CD spectra, whereas a positive peak at 260 nm and a negative peak around 240 nm are associated with a parallel structure.<sup>22,26</sup> In the case of poly(dG)<sub>25</sub>, the presence of a strong maximum at  $\sim$ 260 nm and a shoulder at  $\sim$ 295 nm as well as the negative band at  $\sim$ 240 nm characteristic of a parallel G-quadruplex were observed. This spectrum suggests a polymorphic mixture of G-quadruplex structures that have parallel and antiparallel characteristics.<sup>27</sup>

The addition of **pbg** induced total disappearance of the peak near 260 nm while the peak at  $\sim$ 295 was slightly reduced. In addition, new ICD bands in the 320–400 nm region appeared distinctive of pyrene UV absorption (Fig. 5a). This reveals that the binding of **pbg** more strongly affects parallel G-quadruplex structures. These results were confirmed with G<sub>4</sub>T<sub>4</sub>G<sub>4</sub> which are known to form an antiparallel G-quartet and exhibit a negative band at  $\sim$ 265 nm and a strong positive band at  $\sim$ 295 nm.<sup>22,26</sup> CD spectroscopy confirmed that **pbg** was also able to interact with the anti-parallel G-quartet as evidenced by the appearance of new ICD signals in the 320–400 nm region in a concentration-dependent fashion and a slight decrease in the CD signal at  $\sim$ 295 nm (Fig. 5b).

Finally, we performed studies with poly(rU)<sub>25</sub>, poly(rU)<sub>15</sub> and poly(rN)<sub>25</sub> (5'-AGCUCGUUUAGUGAACCGUCAGAUC-3'), the analogous RNA sequence of poly(dN)<sub>25</sub>. The excimer formation were similar to the one observed with poly(dA)<sub>25</sub> and poly(dA)<sub>15</sub>. Once again, shortening the length of the nucleic acid reduces the exci-

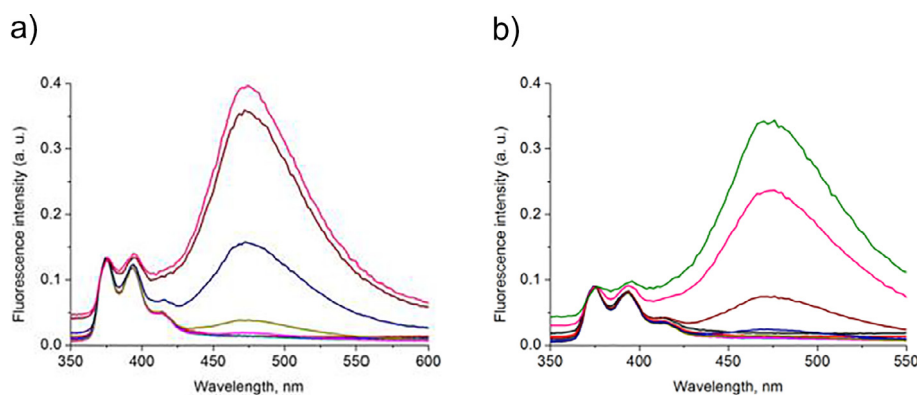


**Fig. 4.** a) Normalized fluorescence spectra of **pbg** (100  $\mu$ M) with a) poly(dG)<sub>25</sub> (0–10.5  $\mu$ M), and b) G<sub>10</sub>T<sub>4</sub>G<sub>10</sub> (0–12.6  $\mu$ M). Experiments were performed in MOPS buffer (1 mM MOPS and 1 mM NaCl) at pH = 7.5.

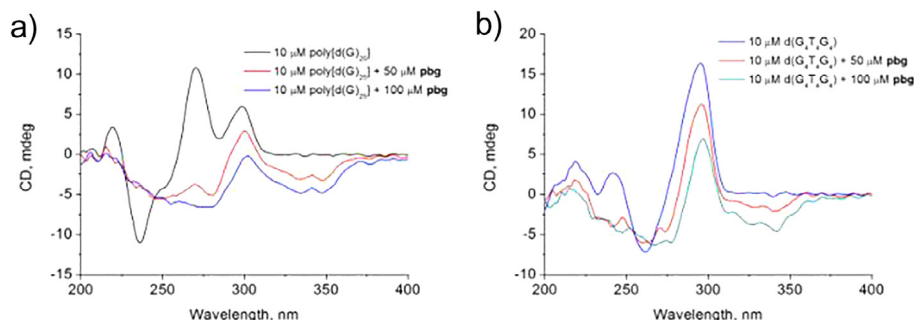


**Fig. 5.** CD spectra of a) parallel quadruplex structure poly(dG)<sub>25</sub> (10  $\mu$ M) and b) anti-parallel quadruplex structure G<sub>4</sub>T<sub>4</sub>G<sub>4</sub> upon the addition of **pbg**. Experiments were performed in MOPS buffer (1 mM MOPS and 1 mM NaCl) at pH = 7.5.

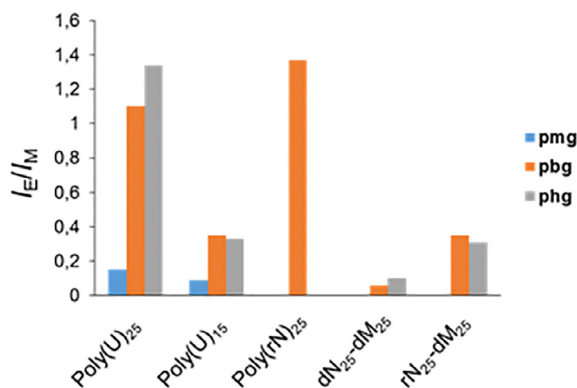


**Fig. 6.**  $I_E/I_M$  maximum values obtained for **pmg**, **pbg** and **phg** (50  $\mu$ M) mixed with various RNA sequences and duplexes. Experiments were performed in MOPS buffer (1 mM MOPS and 1 mM NaCl) at pH = 7.5.

mer formation. Similarly, poly(rN)<sub>25</sub> induced excimer formation in the range of poly(dN)<sub>25</sub>. An interesting observation was made with duplexes. In contrast to poly(dN)<sub>25</sub>-poly(dM)<sub>25</sub> which did not induce significant excimer formation due to intercalation of the pyrene unit into the double helix, as demonstrated by our group in a previous study,<sup>20</sup> poly(rN)<sub>25</sub>-poly(dM)<sub>25</sub> DNA-RNA duplex showed substantial excimer formation (Fig. 6). These results suggest that pyrene molecules do not intercalate into DNA-RNA complexes, and bind outside the duplex, which thus promotes some excimer formation. This hypothesis was substantiated by monitoring induced CD upon the addition of **pbg** to poly(dN)<sub>25</sub>-poly(dM)<sub>25</sub> and poly(rN)<sub>25</sub>-poly(dM)<sub>25</sub>. Indeed, while a significant negative ICD could be observed in the 300–400 nm region in the presence of poly(dN)<sub>25</sub>-poly(dM)<sub>25</sub>, a weaker positive ICD was obtained in the same region with the DNA-RNA hybrid duplex (see Fig. S75).<sup>28,29</sup> These results are also in agreement with a previous report utilizing covalent pyrene-modified oligonucleotides.<sup>30</sup> However, here again no correlation could be made between the number of negative charges of the duplex and the number of positive charges of the guanidinium probe.

In conclusion our results show that positively charged pyrene-guanidinium derivatives are able to induce strong excimer formation upon interaction with different DNAs and RNAs. These oligonucleotides organize the aggregation of pyrene guanidinium derivatives through electrostatic and hydrophobic interactions thus resulting in strong excimer emission. Excimer emission depends significantly on the length of linkage between the pyrene moiety and the guanidinium functionality but also on the DNA structure and sequence. The specific interaction of **pbg** with anti-parallel G-quadruplex structures is reflected by the high excimer formation measured. Pyrene guanidinium derivatives thus comple-

ment the G4 responsive ammonium, imidazolium, and thiazolium moieties reported so far.<sup>10,11,14–16</sup> Considering the importance of G-quadruplex in human telomeres, the optimization and biological evaluation of these compounds will be performed in forthcoming studies.

## Acknowledgments

K.A. thanks the Erasmus Mundus Backis Program for a doctoral fellowship. K.O. acknowledges financial support from the Foundation ARC.

## A. Supplementary data

Supplementary data associated with this article can be found, in the online version, at <https://doi.org/10.1016/j.tetlet.2017.12.046>.

## References

- Nishizawa S, Kato Y, Teramae N. *J Am Chem Soc.* 1999;121:9463–9464.
- Bains G, Patel AB, Narayanaswami V. *Molecules.* 2011;16:7909–7935.
- Karuppannan S, Chambron JC. *Chem Asian J.* 2011;6:964–984.
- Lee MH, Kim JS, Sessler JL. *Chem Soc Rev.* 2015;44:4185–4191.
- Wang CM, Wu CC, Chen Y, Song YL, Tan WH, Yang CJ. *Curr Org Chem.* 2011;15:465–476.
- Ostergaard ME, Hrdlicka PJ. *Chem Soc Rev.* 2011;40:5771–5788.
- Malinovskii VL, Wenger D, Haner R. *Chem Soc Rev.* 2010;39:410–422.
- Ensslen P, Wagenknecht H-A. *Acc Chem Res.* 2015;48:2724–2733.
- Teo YN, Kool ET. *Chem Rev.* 2012;112:4221–4245.
- Zhang RX, Tang D, Lu P, et al. *Org Lett.* 2009;11:4302–4305.
- Yang XY, Liu D, Lu P, Zhang YJ, Yu C. *Analyst.* 2010;135:2074–2078.
- Paolantoni D, Rubio-Magnieto J, Cantel S, et al. *Chem Commun.* 2014;50:14257–14260.
- Zhu ZC, Li WY, Yang CL. *Sensor Actuat B Chem.* 2016;224:31–36.
- Kim HN, Lee EH, Xu ZC, et al. *Biomaterials.* 2012;33:2282–2288.
- Bonsignore R, Notaro A, Salvo AMP, et al. *Chemistryselect.* 2016;1:6755–6761.
- Jiang C, Li LL, Yu XQ. *Anal Methods.* 2017;9:2397–2400.
- Ohara K, Smietana M, Vasseur JJ. *J Am Soc Mass Spectrom.* 2006;17:283–291.
- Ohara K, Jacquinet JC, Jouanneau D, Helbert W, Smietana M, Vasseur JJ. *J Am Soc Mass Spectrom.* 2009;20:131–137.
- Cantel S, Brunel L, Ohara K, et al. *Proteomics.* 2012;12:2247–2257.
- Ohara K, Smietana M, Restouin A, et al. *J Med Chem.* 2007;50:6465–6475.
- Miyoshi D, Nakao A, Toda T, Sugimoto N. *FEBS Lett.* 2001;496:128–133.
- Balagurumoorthy P, Brahmachari SK, Mohanty D, Bansal M, Sasisekharan V. *Nucleic Acids Res.* 1992;20:4061–4067.
- Kaushik M, Kaushik S, Bansal A, Saxena S, Kukreti S. *Curr Mol Med.* 2011;11:744–769.
- Carrasco C, Rosu F, Gabelica V, et al. *ChemBioChem.* 2002;3:1235–1241.
- Randazzo A, Spada GP, da Silva MW. Circular dichroism of quadruplex structures. In: Chaires JB, Graves D, eds. *Quadruplex Nucleic Acids*, Vol. 330:67–86.
- Kypr J, Kejnovska I, Renciuik D, Vorlickova M. *Nucleic Acids Res.* 2009;37:1713–1725.
- Rezler EM, Seenisamy J, Bashyam S, et al. *J Am Chem Soc.* 2005;127:9439–9447.
- Nordén B, Kurucsev T. *J Mol Recogn.* 1994;7:141–155.
- Garbett NC, Ragazzon PA, Chaires JB. *Nat Protoc.* 2007;2:3166–3172.
- Nakamura M, Fukunaga Y, Sasa K, et al. *Nucleic Acids Res.* 2005;33:5887–5895.